Optimal Path of a UAV Engaged in Wind-influenced Circular Towing*

Mariann Merz[1] and Tor Arne Johansen[2]

Abstract— This paper considers the dynamic optimization of the planned path for an Unmanned Aerial Vehicle (UAV) engaged in circular towing of a cable-body system, such that the motion of the towed endmass is stabilized with minimum motion relative to a desired target position. The ultimate research objective is to develop a concept to enable a fixed wing UAV to be used for end body precision positioning maneuvers such as object pickup/dropoff in order to extend the possible range for this type of missions. While solving for the UAV path that minimizes the towed object orbit in the absence of wind or other disturbances is fairly straight forward, obtaining the desired UAV path when subjected to winds is a challenging problem. The main contribution of this paper is to define a robust UAV path planning strategy that results in minimal motion of the towed endbody about a ground-fixed target position.

I. INTRODUCTION

The Norwegian University of Science and Technology (NTNU) are currently researching technologies to allow low-risk missions into remote Arctic maritime aeras, hence are looking to expand the current capabilities of long-range fixed-wing UAVs. The concept illustrated in Fig. 1 involving a circularly towed fixed-wing UAV system is explored for the purpose of precision object placement, surveillance at speeds below minimum UAV speed as well as object retrieval tasks. This approach was demonstrated by missionary Nate Saints who used the technique to deliver gifts and supplies to remote villages in South America in the 1950s [1]. The concept has been further validated for large scale systems through the US Navy program TAke Charge And Move Out (TACAMO), where a rebuilt Boeing 707 is engaged in a high bank angle turn to maintain a near vertical orientation of a long trailing wire serving as a very low frequency antenna.

Obtaining the UAV path that minimizes towed endbody motion is fairly trivial until wind or other upsets destroy the symmetry of the steady-state configuration of the problem. The steady-state solution can be obtained in a number of different ways, including by solving an initial value problem by use of discrete shooting methods, [2], [3], [4], [5], and by solving an optimization problem [6].

Initially, the TACAMO program was plagued with wind-induced vertical (yo-yo) oscillations. Clifton stated that major
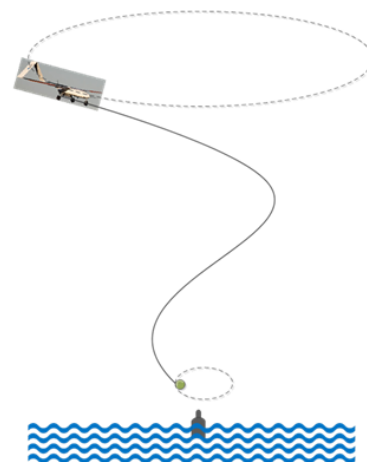

Fig. 1. Concept of Circularly Towed UAV System

updates to the system, such as the use of a smaller gauge wire and the use of a new towing aircraft, caused "wild oscillations" of the wire [7]. In order to minimize the problem, an improved model of the towcable was developed and automatic "Anti yo-yo" control was implemented, where the bank angle was modified as a function of towcable tension and aircraft heading angle [8], [9]. An alternative approach to compensate for the vertical oscillations in winds, involves engaging the towing UAV in a non-constant altitude orbit as suggested in Ref. [10].

In order to successfully manipulate the towed endbody position by means of towing UAV control, it is necessary to recognize the limitations presented by the fact that the manipulations occur via a long highly flexible body. Good accuracy of the endbody motion can only be achieved through use of a fairly accurate towcable model. The complexity of the cable model precludes real-time optimal control methods. A simple strategy is presented where offline optimized control inputs are used to make the towcable attain close to its optimal steady-state shape, followed by regular path adjustments based on the estimated motion of the endbody. This strategy assumes that a fairly accurate estimate of the error between actual and desired position of the towed endbody is available. The main contribution of this paper is the concept for UAV path adjustments in winds, particularly solving for the optimal vertical path using optimal control methods. A path control strategy based on offline optimal control will be shown to greatly reduce the motion of the towed endmass compared to the purely "tilted" path (constant positive/negative vertical velocity when flying with/against the direction of prevailing wind) suggested in [11]. Furthermore,

[1]Mariann Merz is a Ph.D candidate associated with Center for Autonomous Marine Operations and Systems (NTNU AMOS), Department of Engineering Cybernetics, Norwegian University of Science and Technology, Trondheim, Norway mariann.merz@itk.ntnu.no

[2]Tor Arne Johansen is with Faculty of Center for Autonomous Marine Operations and Systems (NTNU AMOS), Department of Engineering Cybernetics, Norwegian University of Science and Technology, Trondheim, Norway tor.arne.johansen@itk.ntnu.no
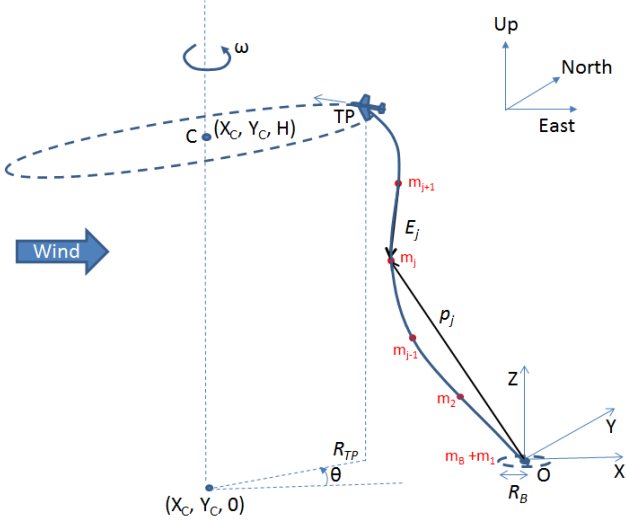
Fig. 2. UAV Towed System Geometries.

Fig. 3.   The Forces Acting on a Point Mass

the work presented here includes a concept for how to adjust the path of the UAV in the horizontal plane to remove the effects from constant winds, to allow the towed endmass to stabilize close to the desired ground-fixed target.

II. MODELLING OF PHYSICAL SYSTEM

Assuming a flat, non-rotating earth, the inertial reference frame is selected as the right-handed coordinate system XYZ, where the X-axis is aligned with the North, the Y-axis points to the East and the Z axis points up. The origin of the inertial frame is O and the unit vectors are $\mathbf{I}$, $\mathbf{J}$ and $\mathbf{K}$ in the X, Y and Z axis respectively. O is assumed to be placed at the target position on the ground where an object should be placed/picked-up. In the presence of a constant wind in the direction of the X-axis (East) previous studies [11], [12], [13] have shown that the desired UAV orbit center must be shifted a significant distance upwind and also slightly to the South for the towed endbody to remain at/near O. The slight shift to the South is due to the fact that the UAV spends much more time flying upwind (West) than downwind (East). The desired orbit center of the towing UAV is labeled C with coordinates (X_C, Y_C, H), and will be updated every orbit based on the estimated position of the towed endbody. Thus, when the towed system is subjected to persistent winds, a local coordinate system at $(X_C, Y_C, 0)$ will translate relative to the inertial system as shown in Fig. 2. The UAV orbit is shown as a circular vertically tilted orbit in the figure, however, the detailed characteristics of the optimal UAV orbit will be determined in the analysis in Section IV. The angle between the horizontal projection of the UAV position vector relative to $(X_C, Y_C, 0)$ and the X-axis is given by θ and the radius of the towing UAV orbit is R_{TP}.

Early research efforts related to the dynamics of towed systems revealed that for scenarios involving a long tow-cable and/or a fairly light weight towed body, the cable dynamics is so dominant that it is necessary to treat the cable as a complete aerodynamic body with properties such
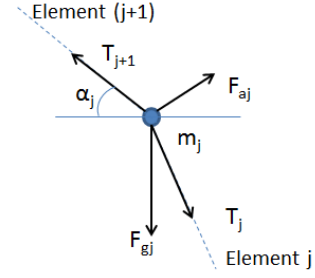
as shape, size, mass distribution and elasticity [16]. The equations of motion for the towing cable are approximated by replacing the continuous cable with a set of N mass points that are connected with massless, elastic thin rods to model stretching of the cable. The point-mass associated with each cable element is numbered from 1 at the towed endbody through N at the towing aircraft attachment point. Lumped Parameter Modelling (LPM) techniques are applied, such that the inertial coupling between cable elements are eliminated by computing the external forces separately for each element. The degrees of freedom of each node are coupled to the neighbors through the tension and strain acting along the connections. It is assumed that the unstrained cable has equal segment lengths (l) between the different point-masses with constant cable diameter (d) and material density ρ_c.

Newton's second law applied to the jth point-mass (m_j) along the towed cable gives:

$$\mathbf{F_j} = m_j \mathbf{a_j}, \quad j = 2, 3, ..., N \tag{1}$$

Similarly, for the bottom cable element with the attached endbody, we have

$$\mathbf{F_B} + \mathbf{F_1} = (m_B + m_1)\mathbf{a_1} \tag{2}$$

$\mathbf{F_B}$ and m_B represents the force and the mass associated with the towed body respectively. The position vector $(\mathbf{p_j})$ of the jth point-mass with respect to the inertial coordinate frame is given by:

$$\mathbf{p_j} = x_j \mathbf{I} + y_j \mathbf{J} + z_j \mathbf{K} \tag{3}$$

A vector representing each cable element can be computed from the positions of the point masses:

$$\mathbf{E_j} = (x_j - x_{j+1})\mathbf{I} + (y_j - y_{j+1})\mathbf{J} + (z_j - z_{j+1})\mathbf{K} \tag{4}$$

The magnitude of this vector represents the stretched length of the element. Once the sum of forces on each element is computed, the accelerations of each lumped mass can be obtained from Newton's second law:

$$\mathbf{a_j} = \ddot{\mathbf{p}}_\mathbf{j} = \frac{\sum \mathbf{F_j}}{m_j} \tag{5}$$

The relevant forces to include in the analysis are the external forces due to the aerodynamic effects $(\mathbf{F_{a_j}})$ and gravity acting on the point masses $(\mathbf{F_{g_j}})$ as well as the internal tension force acting between each of the neigboring

point masses ($\mathbf{T_j}$). Fig. 3 illustrates the forces acting on the jth point mass along the tow-cable. For now, the towed body is modelled as a sphere that generates aerodynamic drag, but no lift. The forces it generates will simply be added to the forces acting on the bottom cable point mass. The detailed derivation and assumptions related to the towcable and endmass forces can be found in Ref. [2].

For the purposes of numerical analysis, reasonable values for a medium sized UAV-towed system and environment were selected and these are summarized in Table 1.

TABLE I

PROPERTIES FOR NUMERICAL ANALYSIS

Parameter	Value	Notes
ρ_a	1.225 kg/m^3	ISA sea-level value. Ignore altitude dependence
$C_{L_{UAV}}$	1.5	Reasonable value for a small UAV
ϕ_{max}	50 deg	A reasonable guess
$V_{UAV_{min}}$	15 m/s	A reasonable guess
$V_{UAV_{max}}$	50 m/s	A reasonable guess
n_{UAV}	$25 kg/m^2$	A reasonable guess
$C_{D_{basic}}$	1.1	Data from Figure 18 in [17]
C_f	0.02	Data from Figure 18 in [17]
C_{D_B}	0.47	Data from Figure 10 in [17]
σ_{UT}	3000 MPa	Honeywell Spectra 1000 Fiber http://www.matweb.com
E	172 GPa	Same as above
ρ_c	970 kg/m^2	Same as above
m_B	2 kg	A reasonable guess
d	0.002 m	A reasonable guess

III. OPTIMAL PATH CONTROL

The towed system is vulnerable to upsets as long as the correction of the towed endmass back to the ground-fixed target has to occur by means of UAV path adjustment via a long flexible towline. Ideally, the towed endmass would be equipped with means of simple control to allow rapid corrections to minor upsets while the towing UAV path control would correct for errors caused by persistent disturbances such as steady winds. It is necessary to allow ample time (at least one UAV orbit) to evaluate the effect of the UAV path adjustments. Borst, Greisz and Quynn [8] state that TACAMO flight tests show that it takes roughly two orbits for the transients from the previous anti-yo-yo adjustment to fully settle such that it is relevant to consider another adjustment. Furthermore, the TACAMO system measures the towcable tension and use this as the primary control feedback parameter, i.e. to minimize the tension oscillation in order to minimize the vertical oscillation. For the purposes of this study, we will assume that we can estimate the position of the towed endmass (possibly by use of a camera or a GPS transmitter) allowing us to use estimated position error as the primary control feedback parameter. However, it is
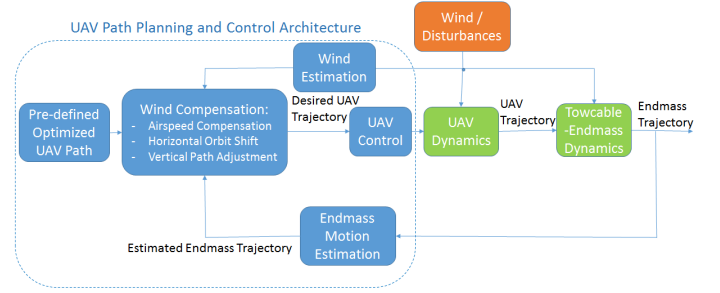

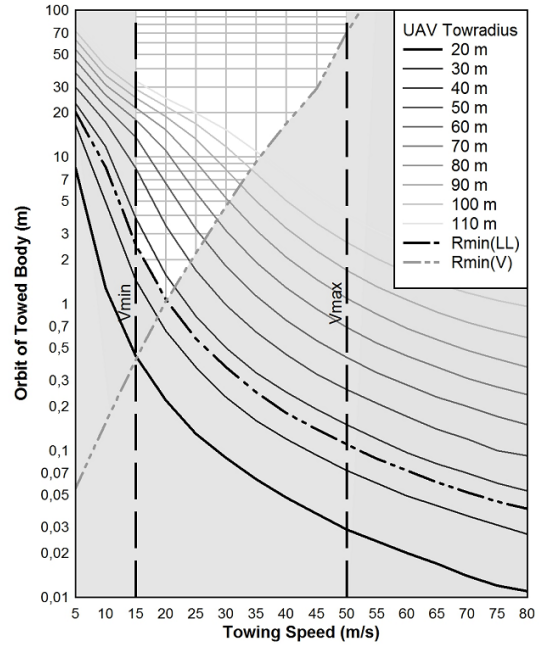Fig. 4. Overview of UAV Path Planning and Control Architecture

Fig. 5. Achievable Towed System Performance with 600 m Towcable [2]

viewed as important to also measure the cable tension at the UAV attachment point to prevent exceeding the ultimate cable strength or allowing the cable from going slack (which could lead to sudden jerks and risk of cable rupture).

An overview of the control strategy for the UAV towed system is shown in Fig. 4.

A. Optimal UAV Path derived for Calm Air

Steady-state configurations for the UAV towed system described in Section II was solved for in Ref. [2] and a summary of the feasible ranges for the control inputs (V_{UAV} and R_{TP}) and the resulting towed endbody orbit is shown in Fig. 5. The figure illustrates the feasible towing configurations for the selected system and clearly identifies the optimal towing configuration that leads to minimal endbody motion.

B. UAV speed control in winds

When the UAV is subjected to winds, the UAV airspeed is no longer equal to its groundspeed. Since the circular towing maneuver requires low airspeeds, and the aerodynamic forces are functions of airspeed, it is important to control to a

constant UAV airspeed that provides a safe margin to stall. The desired UAV velocity vector for path planning ($\mathbf{V_{Path}}$) is the difference between the velocity vector of the UAV relative to a point on the ground ($\mathbf{V_{GP}}$) and the wind vector ($\mathbf{V_W}$):

$$\mathbf{V_{Path}} \; = \; \mathbf{V_{GP}} - \mathbf{V_W} \tag{6}$$

For the setup in Fig 2 we have:

$$\mathbf{V_{Path}} \; = \; (-V_{GP}\sin\theta - V_W)\vec{\mathbf{I}} + V_{GP}\cos\theta\vec{\mathbf{J}} \tag{7}$$

By taking the magnitude of both sides and simplifying, we obtain the following quadratic equation:

$$V_{GP}^2 + (2V_W\sin\theta)V_{GP} + (V_W^2 - V_{Path}^2) = 0 \tag{8}$$

An expression for the desired angular rate ($\dot{\theta}$) in order to maintain constant airspeed in the presence of winds can be obtained by inserting $V_{GP} = \dot{\theta}R_{TP}$ and allowing an arbitrary wind direction ($\theta_c = \theta - \theta_0$):

$$\dot{\theta} = \frac{\sqrt{V_W^2\sin^2\theta_c + V_{Path}^2 - V_W^2}}{R_{TP}} - \frac{V_W\sin\theta_c}{R_{TP}} \tag{9}$$

C. Horizontal Flight Path

The strategy for control of the horizontal path is to shift the UAV orbit upwind such that the motion of the endbody centers about the ground-fixed target, but to keep the orbit parameters (towradius and UAV speed) equal to the optimized values from the no-wind analysis. In practice, the horizontal orbit shift is performed as follows:

1) The estimated position of the towed endbody is used to derive the center of the endbody motion.
2) The position error between the center of endbody motion and the ground-fixed target is computed.
3) The UAV path planner gradually shifts (by limiting the rate of the shift) the desired orbit center of the UAV in accordance with the towed object position error.

Note that this "spiral orbit" scheme can also be employed if a particular mission calls for surveillance at a speed slower than the minimum UAV speed.

D. Vertical Flight Path

The vertical oscillations observed when the towed system is subjected to steady wind, is a result of the geometric asymmetry that develops when the aerodynamic forces acting on the towcable and towed endbody causes these bodies to drift downwind from the path of the orbiting UAV. When the UAV is on the upwind leg of the orbit, the distance to the towed body is greater than when the UAV is on the downwind leg of the orbit. Thus, towcable tension varies over the course of an orbit, and as the towcable is nearly vertical, the result is vertical endbody oscillations. Several ideas to stabilize the tension force have been proposed:

- Use of a high speed cable reel to adjust the towcable length as the aircraft orbits in wind [13]
- Fly a non-constant altitude orbit (inclined) [10], [13]
- Adjust bank angle based on heading relative to wind [8]

For an automatically controlled UAV, the non-constant altitude option is a good choice in terms of simplicity and effectiveness. In [11] simulation results show that by tilting the orbit vertically it is possible to reduce the peak-to-peak oscillation magnitude that the towed system experiences in 3 m/s steady wind from 26 meters to 6.5 meters. For object retrieval missions, reducing the vertical oscillations as much as possible is critical to success. Hence, in the next subsection, an optimal control problem is formulated to solve for the vertical path profile that minimizes the endmass motion.

E. Optimal Control Problem (OCP) - Basic Formulation

A cost function to ensure the endbody motion is minimized can be selected as:

$$J = \int_0^t R_B^2 \; dt = \int_0^t (x_0^2 + y_0^2 + z_0^2) \; dt \tag{10}$$

where t is at least equal to the orbit period. The cost function is subject to the dynamic equations formulated in Section II and is furthermore subject to the following constraints related to UAV maneuver limits and bounds on allowable towline tension:

$$v_{UAV_{min}} \leq \quad v_{UAV} \quad \leq v_{UAV_{max}} \tag{11}$$
$$r_{UAV} \quad \geq \quad \max(r_{min_{LL}}, r_{min_v}) \tag{12}$$
$$T_{min} \quad > \quad 0 \tag{13}$$
$$T_{max} \quad \leq \quad \frac{\sigma_{UT}\pi d^2}{4} \tag{14}$$

Above, $r_{min_{LL}}$ refers to the load limited minimum towing radius which is:

$$r_{min_{LL}} = \frac{2n_{UAV}}{\rho_a C_{L_{UAV}}\sin\phi_{B_{max}}} \tag{15}$$

Here n_{UAV} is the UAV wing loading and $\phi_{B_{max}}$ is the maximum bank angle. Also, r_{min_v} refers to the speed limited minimum towing radius:

$$r_{min_v} = \frac{v_{UAV}^2}{g\tan\phi_{B_{max}}} \tag{16}$$

The limits on the towline tension (T) prevents the towline from going slack and exceeding the ultimate strength (σ_{UT}). Refer to [2] for a more detailed discussion and derivation of the OCP constraints. Solving the basic OCP thus involves determining the optimal control vector ($u = [V_{UAV}, R_{TP}, H]$) such that that the cost function J is minimized and constraints (11) - (14) are satisfied.

Since we do not plan to modify the towing radius or speed for different wind conditions, the optimal UAV airspeed (V_{UAV}) and towing radius (R_{TP}) are known from SS analysis and can be set to fixed values to reduce the size of the OPC.

F. OCP Implementation/Solver Details

To efficiently arrive at the optimal solution to the OCP, numerical optimization software has been employed. The open-source framework CasADi [14] was used in combination with the open-source interior-point NLP solver IPOPT. A single shooting approach was selected for simplicity.
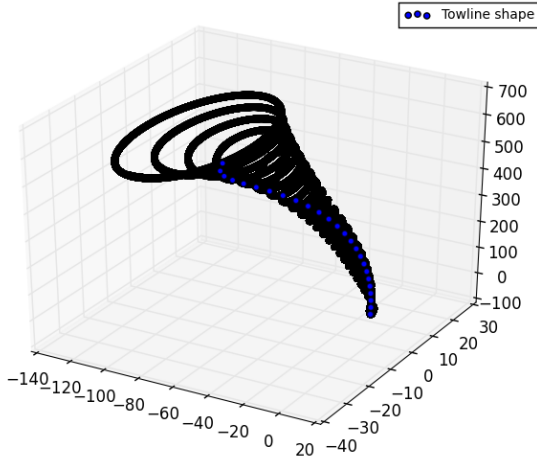
Fig. 6. Profile of the SS Orbit in 3 m/s Wind used for OCP Initial Condition

G. Initial Guess of Cable Shape

In order to converge to the desired solution in a timely manner using single shooting methods, a good guess of the initial cable shape is required. The goal here is to determine the optimal steady-state vertical path given a steady wind, hence the initial condition for the OCP is selected as follows:

- The no-wind steady-state cable shape is obtained using the differentially flat approach described in [2].
- The equations of motion defined in Section II are integrated forward in time, while the wind magnitude is slowly ramped up to the desired value, the UAV orbit is tilted in response to the wind as in [11] and the orbit center is adjusted to stabilize the endmass at the desired ground-fixed point (inertial origin O)
- When the system has achieved steady-state, the cable shape is captured for use in the OCP.

IV. RESULTS

To gain confidence in the method, the OCP was first solved for the basic no-wind towing scenario, which resulted in the same optimal control vector ([20.38, 35.52, 591.79]) as previously obtained from the steady-state analysis in [2].

Next, a steady wind of 3 m/s was added. The initial condition for the this scenario was obtained from a simulation as explained in Section III G, and the orbit profile is shown in Fig 6. In order to successfully solve the OCP formulated in Section III C to derive the optimal UAV orbit profile in constant wind using a regular laptop computer, it was necessary to reduce the number of towcable point masses to 5 (compared to the 25 that was deemed sufficiently accurate in [2]). Note that while the optimal path itself was derived from a 5 point mass cable model, subsequent simulations to verify the resulting performance were made using the 25 point-mass model. Key analysis details are summarized in Table II and the optimal vertical path is shown in Fig. 7.

The dashed line shows a function H_{approx} constructed to closely match the cosine-like shape of the optimal height. A general function to compute a close to optimal UAV height when the system is subjected to steady winds can be taken

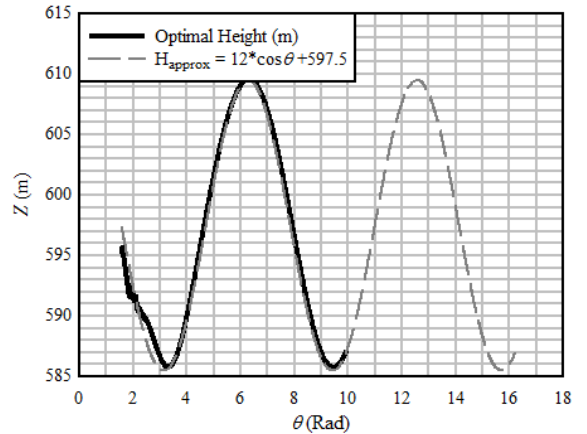| Parameter	Value
Point Masses	5
Time Horizon	15 s
Discretizations	1200
IC Condition	[20.4, 35.5, 585.08]
Optimal Solution	See Fig. 7
Solution Time	203325 s
Number of iterations	54

Fig. 7. Optimal UAV Height in 3 m/s Steady Wind

as:

$$H_{approx} = \Delta H_{max} \cos(\theta - \theta_0) + C_H \qquad (17)$$

The amplitude ΔH_{max} and the centerline C_H of the cosine function can be estimated as functions of the wind magnitude, as shown in Table III.

TABLE III

ΔH_{max} AND C_H FOR A SELECTION OF WIND MAGNITUDES

Parameter	1 m/s	3 m/s	5 m/s
ΔH_{max}	3.0	12.0	24.8
C_H	607.5	597.5	556.5

The Steady-State (SS) orbit formed by the towed endmass resulting from the simulation with a 3 m/s wind and using 25 point masses are shown in Fig. 8, 9 and 10 for the scenario involving no vertical compensation, for a tilted orbit scenario and for the vertical cosine function scenario respectively. The associated vertical oscillation of the endmass is about 26 meters, 5.5 meters and 1.5 meters. Note that all the data have been collected assuming perfect controller tracking.

The success of the control strategy outlined in this paper relies on a way to accurately measure or estimate either the position error of the towed endmass, the wind vector or preferably both these vectors, in order to provide the necessary compensation as detailed in Sections III B, III C and in Table III. The estimation error(s) depends on the instrumentation available onboard the UAV and the endbody (e.g. camera systems, differential GPS, etc). For a small UAV system where no communication link is available
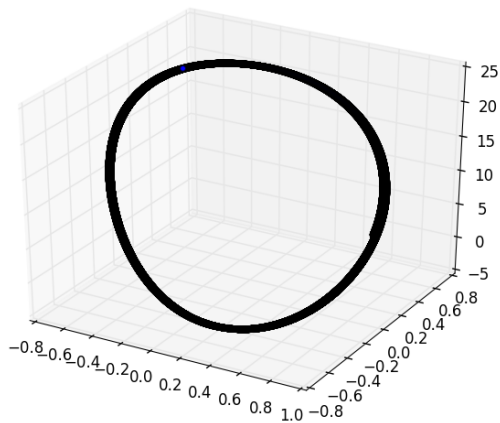
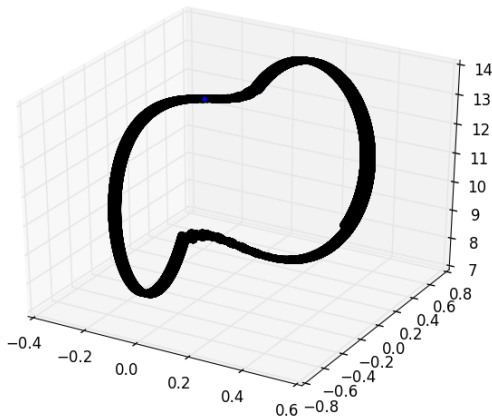Fig. 8.   SS Endbody Orbit given No Vertical Comp. in 3 m/s Wind

Fig. 9.   SS Endbody Orbit given Linear Vert. Comp. (Tilt) in 3 m/s Wind
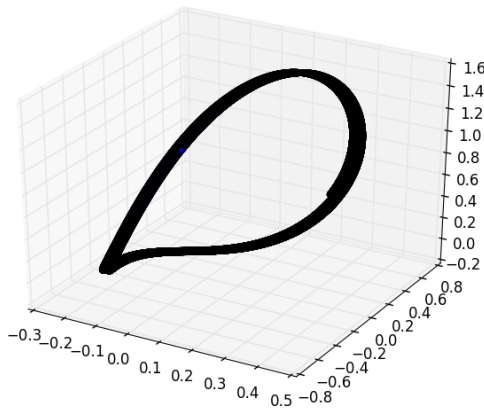

Fig. 10.   SS Endbody Orbit given Cosine Funct. Vert. Comp. in 3 m/s Wind

between the towing UAV and the endmass, deriving sufficiently accurate estimates may be challenging. Future work should consider the benefit of using the tension fluctuations measured at the top of the towline as an additional control input as stabilizing the tension force is directly linked with reducing the vertical oscillations. For the 3 m/s wind scenarios discussed above, the tension for the scenario without any vertical compensation varied between 20 N and 65 N over the course of an orbit while the tension for the scenario using the cosine function vertical compensation varied only

between 33 N and 37 N over the course of an orbit.

V. CONCLUSIONS

A path planning strategy to enable precision control of a circularly towed endbody has been presented. The approach is based on offline determined optimal orbital motion, but where horizontal orbit center shift and vertical path adjustments are performed online using the position error of the towed endbody. Further work could explore if the towline tension force measured at the towline attachment point, is a better choice of control feedback parameter.

REFERENCES

[1] R.T. Hitt *Jungle Pilot: The Gripping Story of the Life and Witness of Nate Saint, Martyred Missionary to Ecuador*, Discovery House Publishers, Updated edition, January 1, 1997
[2] M. Merz and T. A. Johansen *Feasability Study of a Circularly Towed Cable-Body System for UAV Applications*, International Conference on Unmanned Aircraft Systems 2016, Arlington, VA, USA, June 7- 10, 2016.
[3] R. A. Skop and Y.-I. Choo *The configuration of a Cable Towed in a Circular Path* Journal of Aircraft, Vol. 8, No. 11 (1971), pp. 856-862.
[4] J. J. Russell and W.J. Anderson *Equilibrium and stability of a circularly towed cable subject to aerodynamic drag* Journal of Aircraft Vol. 14, No. 7 (1977), pp. 680-686.
[5] J. M. Clifton, L.V. Schmidt and T.D. Stuart *Dynamic modeling of a trailing wire towed by an orbiting aircraft*, Journal of Guidance, Control and Dynamics, Vol.18, No.4, 875-881 (1995)
[6] P. Williams and P. Trivailo *Dynamics of Circularly Towed Cable Systems, Part 1: Optimal Configurations and Their Stability*, Journal of Guidance, Control, and Dynamics, Vol. 30, No. 3, May - June 2007.
[7] J.M. Clifton *Modeling and Control of a Trailing Wire Antenna Towed by an orbiting Aircraft*, PhD thesis (1992), Naval Postgraduate School, Monterey, CA.
[8] R.G. Borst, G.F. Greisz, and A.G. Quynn *Fuzzy Logic Control Algorithm for Suppressing E-6A Long Trailing Wire Antenna Wind Shear Induced Oscillations*, AIAA Guidance, Navigation, and Control Conference, Monterey, CA, USA, August 9-11, 1993.
[9] D.L.J. Brushwood, A.P. Olson, and J.M. Smyth *The E-6A Orbit Improvement System and its Effect Upon LTWA Verticality*, Guidance, Navigation, and Control Conference and Exhibit, Boston, MA, USA, 1998.
[10] J.G.R. Hansen, S.A. Crist *Dynamics of Cables Towed from Aircraft*, United States Airforce Academy, Research report 72-8, October 1972.
[11] M.Merz and T.A. Johansen *A Strategy for Robust Precision Control of an Endbody being Towed by an Orbiting UAV* AIAA Guidance, Navigation, and Control Conference, Grapevine, Texas, USA, January 8 - 12, 2017.
[12] R.M. Murray *Trajectory Generation for a Towed Cable System using Differential Flatness*, IFAC Word Congress, San Francisco, July 1996.
[13] P. Williams *Optimization of Circularly Towed Cable System in Crosswind*, Journal or Guidance, Control, and Dynamics, Vol. 33, No. 4, July - August 2010.
[14] J. Andersson *A General Purpose Software Framework for Dynamic Optimization*, Arenberg Doctoral School, KU Leuven, 2013 PdD Thesis, Dept. of Electrical Engineering (ESAT/SCD) and Optimization in Engineering Center, October. Kasteelpark Arenberg 10, 3001-Heverlee, Belgium.
[15] M.B. Colton, L. Sun, D.C. Carlson and R.W. Beard *Multi-vehicle dynamics and control for aerial recovery of micro air vehicles*, Int. J. Vehicle Autonomous Systems, Vol.9, Nos. 1/2, pp. 78 - 107, 2011.
[16] W. H. Phillips *Stability of a body stabilized by fins and suspended from an airplane*, NACA Wartime Report L-28, 1944.
[17] S.F. Hoerner *Fluid Dynamic Drag*, Published by the Author, 1965